

RESEARCH ARTICLE

Evaluation of the emission inventory for large point emission sources in South Korea by applying measured data from the NASA/NIER KORUS-AQ aircraft field campaign

Minwoo Park¹, Hyejung Hu², Younha Kim³, Alan Fried⁴, Isobel J. Simpson⁵, Hyungah Jin⁶, Andrew Weinheimer⁷, Greg Huey⁸, James Crawford⁹, and Jung-Hun Woo^{2,10,*}

One of the major issues in determining a region's air quality is the uncertainty of large point sources (LPSs) emissions, which significantly affect the local-regional air quality. In this study, the SO₂ and NO_x emissions of 5 major LPSs in South Korea were evaluated by comparing the emissions-based concentrations employing a Gaussian dispersion model with aircraft-based measurements from DC-8 "around-the-stack" flights through the National Aeronautics and Space Administration (NASA)/National Institute of Environmental Research (NIER) KOREA-U.S. Cooperative Domestic Air Quality (KORUS-AQ) aircraft field campaign. The ratio between modeled and measured concentrations for all 5 LPSs ranged between 0.42 and 1.30 and 0.39 and 1.01 for NO_x and SO₂, respectively. The results for the Boryeong, Dangjin, and Seocheon power plants (PPs), where the locations and sizes of stacks are easier to specify than industrial complexes (Hyundai Steel and Hankook Glass), yielded better performance, which ranged between 0.82 and 1.30 and 0.79 and 1.01 for NO_x and SO₂. This level of agreement was very encouraging, considering that the modeled concentrations were based on 30-min averaged emissions compared to less-than-a-minute DC-8 around-the-stack measurements. Based on our analysis, the uncertainty of LPS emissions, at least for NO_x and SO₂, appears to be small, which implies that the point sources inventory emissions are reasonably accurate. The Dangjin PP's analysis reveals that the actual measured emissions should be considered in addition to "the official" inventory amounts to reduce emission uncertainty. This detailed comparative analysis verified the method used for this study. The findings of this study are expected to enhance the performance of future LPS emission inventory assessments. In terms of recommendations, the data from the raw emission inventory should include more clear information about the locations of measured stacks to obtain more accurate emission estimates. In addition, the flight measurement duration should be long enough to fly around several times to reduce uncertainties, and the flight positions and altitudes should be varied. By improving LPS inventories through accurate evaluations, more accurate air quality forecasts and better policies could be made. As a result, it is expected that public health can be improved by reducing the time people are exposed to high concentrations of air pollutants.

Keywords: CAPSS emission inventory, NASA/NIER KORUS-AQ aircraft field campaign, Large point source, Emission evaluation

1. Introduction

It is well-known that industrialization and population growth are directly related to increasing emissions of air pollutants. Asia, particularly northeast Asia such as South

Korea, Japan, and China, has had rapid population growth and industrialization in the last several decades and has been suffering from severe air pollution problems (Crippa et al., 2018; Kurokawa and Ohara, 2020). Although the

¹Department of Advanced Technology Fusion, Konkuk University, Seoul, Korea

²Department of Technology Fusion Engineering, Konkuk University, Seoul, Korea

³International Institute for Applied Systems Analysis, Laxenburg, Austria

⁴INSTAAR, University of Colorado, Boulder, CO, USA

⁵University of California, Irvine, Irvine, CA, USA

⁶NIER, National Institute of Environmental Research, Seoul, Korea

⁷National Center for Atmospheric Research, Boulder, CO, USA

⁸Georgia Institute of Technology, Atlanta, GA, USA

⁹NASA Langley Research Center, Hampton, VA, USA

¹⁰Department of Civil and Environmental Engineering, Konkuk University, Seoul, Korea

* Corresponding author:
Email: jwoo@konkuk.ac.kr

amount of emission varies depending on the type of pollutant, it was reported that about 20%–35% of the global air pollutants were emitted in this region (Klimont et al., 2017; Crippa et al., 2019). Because the hazardous nature of air pollutants to human health is well documented, many countries in northeast Asia including Korea have been making great efforts to reduce air pollution emissions.

In Korea, various air pollution reduction policies have been implemented mainly in the Seoul metropolitan area (SMA), including Seoul, Incheon, and Gyeonggi. Even though the total area of SMA (12,685 km²) is 12.6% of Korea, SMA accommodates half of the population of Korea (Statistics Korea, 2020). Consequently, more than half of the vehicles in Korea, which are one of the main sources of air pollution in urban areas, are operated in Seoul. Therefore, SMA is undoubtedly the area where air pollution reduction policies need to be implemented intensively. Moreover, as public awareness of fine particles among various air pollutants increases, more effective policies to reduce the concentration of fine particles are required. Here, fine particles are also known as PM_{2.5} (particulate matter below or equal to 2.5 μm in aerodynamic diameter) and those with even smaller diameters are called ultrafine particles. These are well-known as high-risk elements to human health, and they have become a big concern because days with a high concentration of fine particles appear frequently in the SMA (Yeo et al., 2019).

Many researchers have made efforts to understand the high concentration of air pollutants in the SMA and have pointed out that in addition to sources such as automotive emissions, pollutants from domestic large point sources (LPSs) and pollutants transported from abroad can also be important (National Institute of Environmental Research [NIER] and National Aeronautics and Space Administration [NASA], 2017; NIER and NASA, 2020). This research suggests that it is essential to consider the effect of domestic LPSs emissions in order to estimate the concentration of air pollutants. For instance, coal-fired power plants (PPs), which fall in the LPSs category, exert a large influence on the generation of secondary ultrafine particles by emitting not only nitrogen oxides (NO_x) but also sulfur dioxide (SO₂). Kim et al. (2016) and Park et al. (2020) described that fine particles transport from the LPSs on the mid-west coast of Korea considerably contributed to the air pollution of the SMA. Kim et al. (2017c) also suggested reducing the influence of LPSs in Chungcheongnam-do, a province located on the mid-west coast of South Korea, to reduce the concentration of fine particles in the SMA. In addition, many studies described the significant contribution of pollutants transported from abroad to the air pollutants in Korea. Since the geographical location of South Korea is westerlies area (Kim, 2019), the concentration of air pollutants in Korea has been greatly influenced by long-range transport from emissions from China as well as Korean-generated domestic emissions (Kim et al., 2012; Lee et al., 2017; Kim et al., 2021a). To this end, distinguishing domestic emissions sources from out-of-region upwind sources has become a very important research area to understand the current efforts to improve air quality over South Korea (Kim et al.,

2017a). In order to establish effective countermeasures against the fine particle problem, one first requires a better understanding for the domestic emission sources and abroad emission sources, when estimating the concentration of air pollutants.

This research focuses on the domestic emission sources related to LPS emissions. Specifically, the primary goal of this study is to evaluate the estimated LPS emission inventories. In Korea, data on LPS emission source types and emission rates are stored and managed in the Clean Air Policy Support System (CAPSS), which is the national emission inventory of Korea (Lee et al., 2011b). In Korea, there are not many studies evaluating the emission inventory, and there are even fewer studies evaluating the LPS emission inventory. In this study, the emissions inventory of selected 5 LPSs on the mid-west coast of Korea was evaluated. The selected LPSs are 3 PPs in Dangjin, Seocheon, and Boryeong; the Hyundai steel mill in Dangjin; and the industrial complex in Gunsan. The Gaussian plume model (GPM) was used for dispersion analysis to estimate the downwind concentrations of NO_x and SO₂ for the selected LPSs. NO_x and SO₂ emitted from LPSs greatly influence the generation of secondary ultrafine particles. The best available bottom-up emissions from the CAPSS and the CleanSYS (also known as continuous emissions monitoring system [CEMS]) were assessed in this study employing measured meteorological and trace gas concentration data acquired from the NASA DC-8 aircraft during the 2016 KORUS-AQ study. Bottom-up inventory results were compared with concentrations measured from the circular flight tracks around emission sources by the DC-8 aircraft. The methods of assessing the reliability of the LPS emission inventory and analysis results are described in the following sections.

2. Identified research points

Many kinds of research have been carried out to improve emission inventories using measured concentrations. In Korea, Kim et al. (2009) targeted the whole country, and Jo and Kim (2015) focused on specific areas in their emission evaluations. The effect of emissions on air quality was assessed by sectors in the CAPSS inventory in the Kim et al. (2009) and Lee et al. (2009) studies. Carotenuto et al. (2018) and Lavoie et al. (2015) evaluated the LPS emissions using aircraft measurements. After the 6-week spring 2016 KORUS-AQ project was carried out, studies related to aircraft measurement-based inverse emissions estimation were conducted by NIER and NASA (2020), Fried et al. (2020), and Simpson et al. (2020). Fried et al. (2020) calculated mass emission rates for various VOCs and formaldehyde from the Daesan petrochemical complex using DC-8 data employing a mass balance approach. Simpson et al. (2020) characterized the VOC emission signatures from the Daesan petrochemical complex and contrasted them with VOC signatures from Seoul and from air arriving from China. The KORUS-AQ campaign was conducted between April and June 2016, and air pollutants were measured from several research aircrafts' measurement. However, in these previous emission

inventory evaluation studies, the characteristics of individual emissions source could not be comprehensively determined because annually averaged emissions were calculated from selected days of aircraft data for comparisons with the annual emission inventory data. As noted in these studies, the snapshot aircraft determinations may not accurately reflect the true LPS emissions averaged over the year. Therefore, to estimate the emissions from specific LPSs at the time of measurement for comparisons with aircraft measurements, a bottom-up emissions inventory for that specific time period and specific LPS was needed. In this study, the CAPSS and the CleanSYS represent the data sources for acquiring bottom-up emissions for these targeted 5 LPSs.

In this study, actual concentrations measured by DC-8 aircraft flying a circular path around the emission sources were used for cross-comparison with modeled concentrations using GPM at targeted LPSs. The flights were made according to the KORUS-AQ aircraft field campaign in 2016 (Crawford et al., 2021). The KORUS-AQ project was performed to study the air quality of Korea and East Asia in relation to chemical evolution, emission inventories, transboundary contributions, and future satellite-based studies of air pollution. The DC-8, the aircraft used for measuring pollutant concentration and meteorological data in this study, was the largest airborne platform among the 3 aircrafts participating in the KORUS-AQ campaign. Through various instruments mounted on the DC-8, it was possible to sample trace gases such as ozone and NO₂ and aerosol composition. This large airborne platform had the added advantage that important meteorological factors such as wind speed, wind direction, and atmospheric pressure were all measured at the same time as the trace gas and aerosol measurements.

Various chemical transport models (CTMs) such as Weather Research and Forecasting model coupled with Chemistry (Grell et al., 2005), Community Multiscale Air Quality (Byun and Ching, 1999), and so on have been used for estimating concentrations in evaluating emission inventories. The estimated concentrations from these CTMs were compared with the results of satellite observations or ground-based measurements (Kim et al., 2013; Han et al., 2015; Goldberg et al., 2019). In previous studies, Brute-force method was used to evaluate each pollutant source, material, and contribution in the SMA (Kim et al., 2017b). However, because model-ready emissions for CTM inputs are spatially gridded and based on the annual emissions inventory, these CTMs are not suitable for modeling emissions dispersion at a specific location during the short time period for the KORUS-AQ study.

Therefore, in this research, the GPM was selected for the dispersion modeling. The GPM dispersion model is based on the normal distribution curve and is the most common dispersion model for estimating the concentration at specific point sources (Awasthi et al., 2006). The GPM was considered the most appropriate model for estimating and comparing point-to-point measurements at flight altitude while considering the nature of the emissions of the LPS stacks. This model has the characteristic of simulating only steady state. To compensate for this, average input factors were prepared using the values measured while flying

around the stacks in a circular pattern aboard the DC-8 during KORUS-AQ. Through this process, it was possible to build the input data for the model that can simulate the situation at the measurement times as much as possible.

In this study, bottom-up emission values from CAPSS and CleanSYS and meteorological data from KORUS-AQ were applied as factors in the GPM. The model was used to calculate the theoretical concentration of the pollutant in areas over which the DC-8 passed for the comparison with the measured value. The comparison of modeled and measured concentrations provides a more comprehensive understanding of the LPS emission inventory. One of the goals of this study was to identify factors to be considered in emissions estimation modeling for more accurate concentration estimation, more reliable air pollution forecasting, and more effective air quality policymaking.

3. Analysis method

3.1. Selected dispersion model

The GPM was used to estimate concentrations of NO_x and SO₂ for this research. The GPM equation (Overcamp, 1982) is shown as follows:

$$C(x, y, z; H) = \frac{Q}{2\pi u \sigma_y \sigma_z} \exp\left[-\frac{y^2}{2\sigma_y^2}\right] \left\{ \exp\left[-\frac{(H_e - z)^2}{2\sigma_z^2}\right] + \exp\left[-\frac{(H_e + z)^2}{2\sigma_z^2}\right] \right\} \exp^{-kt}. \quad (1)$$

The concentration (C , in $\mu\text{g m}^{-3}$) of a pollutant at a location (x, y, z, H) is controlled by variables including wind speed (u), the dispersion coefficient (σ_y and σ_z), and the effective stack height (H_e), which is the sum of the physical height of the stack and the plume rise height. However, the GPM does not take into account the density of individual molecules. In Equation 1, Q represents the emission of the pollutant (as $\mu\text{g s}^{-1}$) and u represents the wind speed (m s^{-1}) at the stack height H . σ_y and σ_z are the dispersion coefficients in the y and z directions (units of m), which are the indicators of dispersion at distance x . The unit of $x, y,$ and z is meters. The effective stack height H is an indicator of how much the air pollutants from the stack rise in the vertical direction due to the emission temperature and the mechanical energy. k indicates the reaction rate of each pollutant with the hydroxyl radical (OH) and t is the transport time (s).

In this study, the transport time t was calculated by dividing the distance between a given stack and the location of DC-8 by the wind speed (Overcamp, 1982). The reaction rate of NO_x and SO₂ was calculated by applying values from several previous studies (Lee et al., 2011a; De Foy et al., 2015; Fioletov et al., 2015; Liu et al., 2016; Shah et al., 2020).

3.2. Inputs for the dispersion model

Figure 1 illustrates the overall analysis method used to evaluate the LPS emissions in this study. There are 3 categories of input data in the GPM: emission inventory, inputs for plume rise estimation, and dispersion

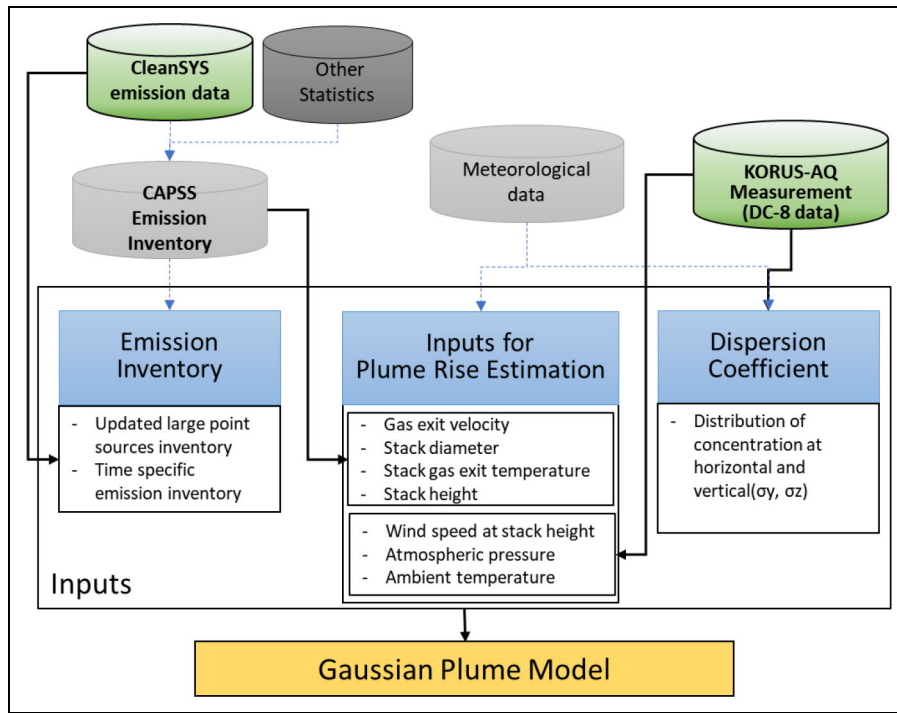


Figure 1. Inputs for the Gaussian plume model (GPM). Dotted lines: Connections between inputs used in the existing studies and inputs for the GPM. Bold solid lines: Connections between newly used sources in this study and inputs for the GPM.

coefficients. The dotted lines present the connections between the input sources used in the existing studies and the inputs for the GPM. The bold solid lines show the connections from the newly used sources in this study.

3.2.1. Emission inventory

The emission inventory for the GPM was derived from the CAPSS inventory. CAPSS is the national emission inventory of South Korea developed by the NIER (2019). Since CAPSS provides annual emissions in the inventory, the CleanSYS stack emission measurement data, which are raw emissions of CAPSS, were used to estimate at-that-time emissions of the selected LPSs. More detailed information about CAPSS emission inventory and LPSs emissions are shown in Figure S1.

The emissions used in this study are based on CleanSYS, also known as CEMS, in Korea, 2016. Because the LPSs used in this study are equipped with CEMS, they transmit wirelessly monitored emissions data to the CleanSYS. The stack emissions measured as concentrations are converted to mass amounts ($\mu\text{g m}^{-3}$) in the CleanSYS and then aggregated in the CAPSS emission inventory. Since the emission data of CleanSYS were provided every 30 min, in this study, values that corresponded to 30-min intervals of time during which the DC-8 flew were used. The CleanSYS-based LPS emissions are treated as being more reliable than annual fuel activity-based emissions (Jang et al., 2009). Because the annual emissions for each LPS from the CAPSS were provided by combustion source type and industrial process types, this information was used for distributing emissions to each selected stack by considering the fuel types of the LPSs.

3.2.2. Inputs for plume rise estimation—Stack parameters

The CAPSS inventory contains comprehensive information about the stacks built in various industries, including specific details such as the dimensions of the stack and the type and amount of pollutants emitted. Additionally, the CAPSS inventory provides important input parameters for the plume rise model, including stack parameters such as gas exit diameter, gas exit velocity, and gas exit temperature.

3.2.3. Inputs for plume rise estimation—Meteorological parameters

To run the GPM with measurement-driven data, meteorological parameters such as temperature, wind direction, and speed measured from the DC-8 aircraft during KORUS-AQ were used to calculate plume rise. Information on meteorological data from DC-8 used in this study is available at https://asdc.larc.nasa.gov/project/KORUS-AQ/KORUSAQ_MetNav_AircraftInSitu_DC8_Data_1. Crawford et al. (2021) contain information about the KORUS-AQ campaign and discuss the measurement equipment used during the campaign, as well as the meteorological data collected from the DC-8 aircraft. Using the measured values, we expected to simulate the situation as realistically as possible at the time of measurement. The following equations were used to calculate effective stack heights and wind speed at the stack height from measured meteorological data from the DC-8.

Equation 2 represents the Holland formula (Holland, 1953; U.S. Environmental Protection Agency, 1974), which was used to calculate effective stack heights based on the meteorological parameters extracted from the DC-8 data,

where ΔH is the plume rise (m), u_h is the wind speed at stack height (m s^{-1}), V_s indicates the emitting velocity, d_s represents the diameters of each stack (m), P_a is the ambient pressure (millibar), T_s is the stack gas temperature (K), and T_a indicates the ambient air temperature (K)

$$\Delta H = \frac{V_s d_s}{u_h} \left\{ 1.5 + 2.68 \times 10^{-3} \times P_a \left(\frac{T_s - T_a}{T_s} \right) \right\}. \quad (2)$$

Equation 3 was applied to convert airborne wind speed measurements into wind speed at the stack height. In this equation, U indicates velocity at stack height (m s^{-1}), U_{ref} denotes the velocity measured by the aircraft (m s^{-1}), Z represents the stack height (m), Z_{ref} is the aircraft altitude (m), and the coefficient n shows the stability of the atmosphere (Davenport, 1961; Touma, 1977)

$$U = U_{\text{ref}} \times \left(\frac{Z}{Z_{\text{ref}}} \right)^n. \quad (3)$$

3.3. Dispersion coefficient

In the Gaussian dispersion model, the dispersion coefficient is a measure of the extent to which the emissions from the source are diffused along their path to the measurement point. In this study, the dispersion coefficients of the LPSs were extracted from the KORUS-AQ air pollution measurement data.

The scheme suggested by Martin (1976) was used to calculate the dispersion coefficients according to the atmospheric stability and distance of each LPS target source. The related variables are shown in Table S1.

4. Data analysis

4.1. Study sites

The KORUS-AQ campaign was jointly conducted by the NIER in Korea and the NASA in the United States, in 2016. One of the purposes of this campaign was to better understand the factors controlling air quality and to provide guidance on measures to improve air quality in Korea (NASA, 2017). As stated in Section 2, this campaign was conducted between April and June 2016 and measured pollutant concentrations using research aircraft (DC-8 and B-200), ground sites, ships, and satellites (NASA, 2020).

During the KORUS-AQ campaign, 23 flights were conducted in total, each with a different goal, such as measuring the concentration of air pollutants arriving from China by intensively flying over the West Sea or checking the magnitude of emissions from traffic and other sources by intensively measuring emissions over SMAs. One of the mission goals was evaluating emission inventories for some LPSs, employing the flight tracks over the mid-west coast of Korea, as shown in **Figure 2**. While the DC-8 repeatedly flew over the facilities in circular patterns, atmospheric sampling and meteorological data measurements near the LPS were performed. The concentrations of pollutants measured by the DC-8 on June 5, 2016, when the mission goal was evaluating LPSs emission, were used to validate the emission inventory. In this study, we focused on to use June 5 flight data, because there are little and short measured data from other flights that

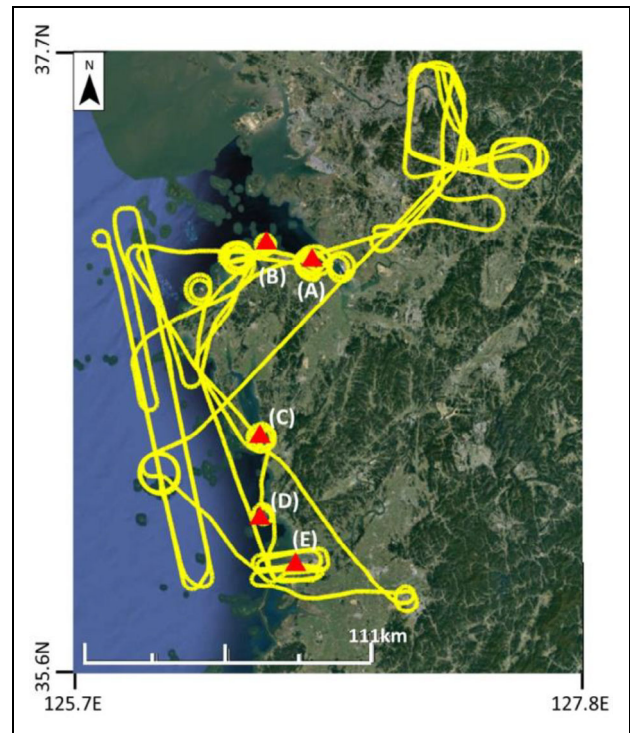


Figure 2. Flight path of the DC-8 on June 5, 2016, and selected large point sources. (A) Hyundai steel mill, (B) Dangjin power plant (PP), (C) Boryeong PP, (D) Seocheon PP, and (E) Gunsan Industrial Complex (HanGlas).

passed through selected LPSs. The triangular symbols in red in **Figure 2** show the locations of selected LPSs, such as large industrial complexes and coal-fired PPs.

As shown in **Figure 2**, the selected LPSs are the Dangjin, Seocheon, Boryeong PPs, the Hyundai Steel, and the Gunsan Industrial Complex (GIC) HanGlas. The sampling locations and time periods for each LPS are listed in Table S2. All times in this article refer to local times.

Figure 3 contains the satellite images of the 5 LPSs, which shows the locations of stacks in each LPS. It was assumed that the point source emissions were at the locations of the corresponding stacks. By checking the locations of visible stacks and flight paths of each LPS, the “effective stacks” that affect the concentrations captured by the airplane were defined. The stack, which was judged not to influence the airplane measurement, was marked with an “X” symbol in (A) and (C) panels of **Figure 3**.

A brief description of each LPS is as follows:

- (A) Hyundai Steel: It is one of the largest steel mills in South Korea and the 13th largest in the world. About 1 min of data extracted from the DC-8 at 11:27 AM was used for the following analyses. We only used a portion of circular measurements because we ran a plume model. So, only enhanced concentration of measurement in the downwind part was used for intercomparison. Hyundai Steel’s stacks are distributed irregularly, while the stacks of other coal-fired PPs are gathered in one place. Therefore, the uncertainty of the modeled plume concentration is expected to increase.

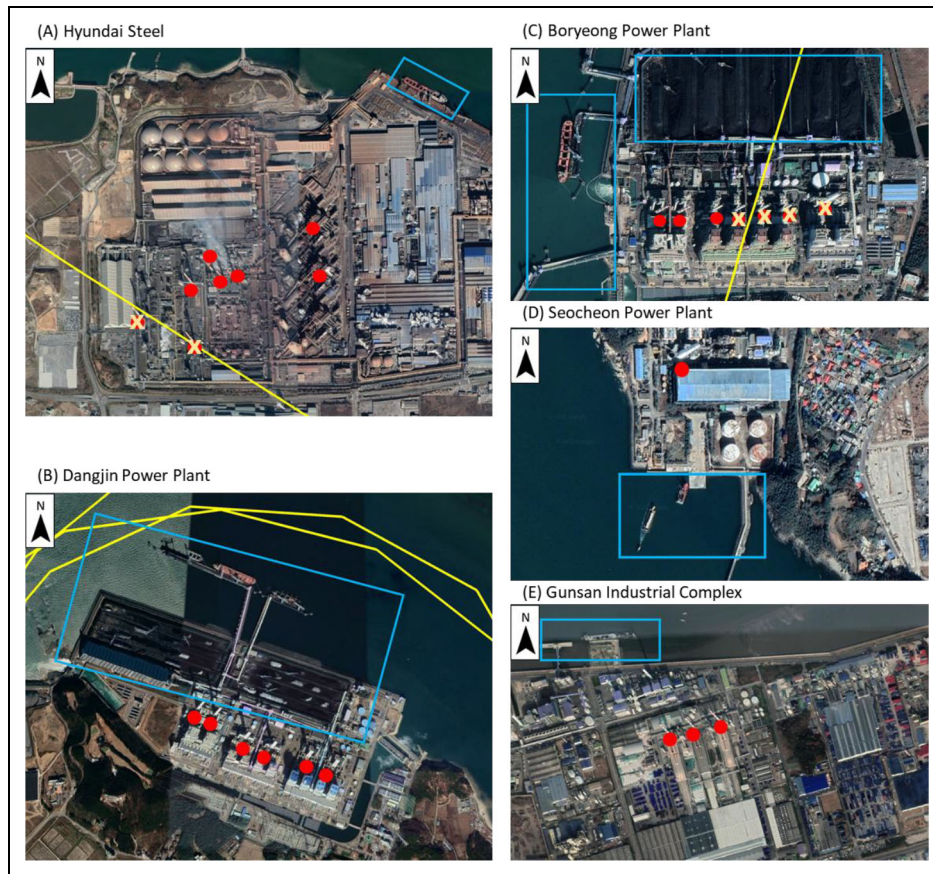


Figure 3. Aerial photography of the 5 large point sources. The red dots mark the large stacks seen from the satellite images. Satellite image source; Google Earth Pro 7.3.4.8248. (A) Hyundai steel, (B) Dangjin power plant, (C) Boryeong power plant, (D) Seocheon power plant, (E) Gunsan industrial complex.

- (B) Dangjin PP: It is the third largest coal-fired PP in the world and the second largest in South Korea. Concentration comparisons between the modeled values and the measured values were conducted using the collected data from 3 flight paths. **Figure 4** depicts the location of the 3 measured points (BF1, BF2, and BF3). There are multiple stacks in Dangjin PP, but distances from stacks are averaged in this figure. Measured data at 2:45 PM were used for BF1 (Dangjin Flight 1) and BF2, and data at 2:50 PM were used for BF3.
- (C) Boryeong PP: It is Korea's largest PP and the second largest coal-fired PP in the world in 2016. This coal-powered generator provides about 6% of all domestic power in South Korea. The DC-8 flew directly above the stack of the Boryeong PP, and about 1 min of data collected at 2:03 PM was used.
- (D) Seocheon PP: It is a relatively small PP with only 2 small power generators and a capacity of 200 MW. The DC-8 flew around the PP twice. The inner circle flight was selected to minimize uncertainty because the outer flight path was about 1.7 km away from the stacks. From this flight, about 1 min of data at 1:47 PM was taken.
- (E) GIC (HanGlas): It is located in the Jeollabuk-do province. In the past, concentrations measured at the ambient air quality monitoring stations in this area have not matched well with the emissions

inventory-driven modeled concentrations. However, the measurements of the fine particle gauges often show “bad” levels ($36 \sim 75 \mu\text{g m}^{-3} \text{ day}^{-1}$; AirKorea, 2020), suggesting that Jeollabuk-do emissions might be underestimated. This could be, however, due to external factors, such as transboundary influences from China or unidentified local emission activities (Kim et al., 2021b). In any event, the emissions of the largest emitter in Jeollabuk-do area, the Gunsan Industrial Complex (E), are in need of evaluation. Roughly 1 min of data at 10:24 AM was used.

Blue squares in **Figure 3** indicate the locations of other emission sources besides the selected LPSs, including area and mobile sources such as fugitive emissions from ships or construction machinery. Although it cannot be said that these sources did not affect the measured concentration, they are not included in emission estimations in this study. As shown in Table S3, the average altitude of the DC-8 flying around the stacks was about 350 m for all 5 LPSs. It was expected that emissions plumes rising from the area and mobile sources could not reach that height (Brunner et al., 2019).

4.2. Emission inventory and emission adjustment

CAPSS provides an annual emissions inventory, and the CleanSYS continuously measures stack emissions data 24

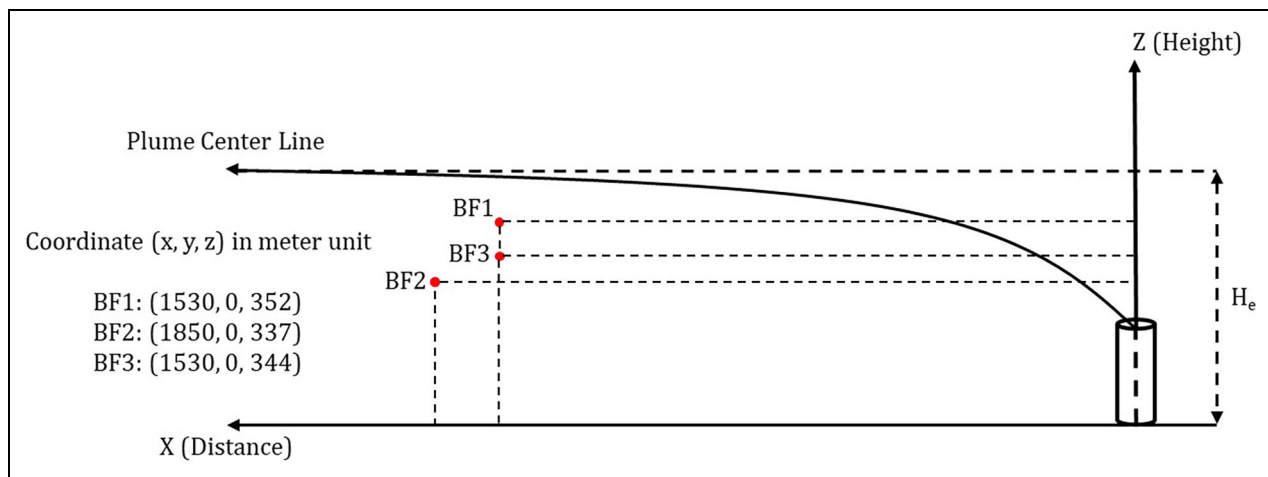


Figure 4. Dangjin PP flight position on plume centerline. x = Downwind distance from stack, y = horizontal distance from center line, and z = flight altitude of aircraft.

h a day, every day. Therefore, CleanSYS data were appropriate to acquire the emissions of the selected LPSs for the time point of the DC-8 flight on June 5.

NO_x and SO_2 emissions of the sampling time points for each LPS were collected from the CleanSYS. The CleanSYS provides emissions for individual stacks, but not the location of each stack. Therefore, some efforts to estimate emissions from effective stacks were required. First, effective stacks need to be defined. In **Figure 3**, the red dots presented visible large stacks. Among those, effective stacks are what directly affect the concentrations along the flight paths. By checking the locations of visible stacks and flight paths of each LPS, the effective stacks were defined, which are summarized in **Table 1**. Second, the emissions of each LPS could be adjusted by considering fuel types used in effective stacks. It was possible to guess the fuel types in effective stacks by checking the facility information. The annual emissions for each LPS from the CAPSS were provided by combustion source type and industrial process types. This information such as ratios by source classification code types was used for emission adjustment. The adjusted NO_x and SO_2 emissions for each LPS are also summarized in **Table 1**.

According to the specific characteristics of facilities, NO_x and SO_2 emissions for the 5 LPSs are calculated. Modifications are described in detail in the following:

- (A) Hyundai Steel: It is spatially divided into (A-1) shaft furnace area and (A-2) electric furnace area as shown in **Figure 5A**. Facilities for making iron and steel and so on are located in the A-1 area. Facilities for making alloy steel and rebar making and so on are in A-2. Because 6 effective stacks are in the (A-1) shaft furnace area, emissions from bituminous coal and liquefied natural gas (LNG) usage were included. The emissions from (A-1) area accounted for 97% of NO_x and 95% of SO_2 of all Hyundai Steel emissions. The ratios were acquired from the CAPSS inventory and applied to modify the emission input from the CleanSYS emissions.

- (B) Dangjin PP: In December 2015, the construction of new coal power facilities (9th and 10th) of the Dangjin PP was completed. The year 2016 was the period for stabilization of the new facilities, to solve the initial operational problems, and commercial operations started in January 2017. During this stabilization period in 2016, KORUS-AQ proceeded to measure the emissions of Dangjin PP. Emissions from the pilot operations were measured but not reported to the CleanSYS. This situation was handled by adding the possible emissions from the pilot operations from Facilities 9 and 10 and excluding emissions from Facility 1, which has been shut down since May 2016. All emissions from the Dangjin PP assume that the existing Units 2–10 were operational (Korea East-West Power Company, 2020). Emissions of the added Facilities 9 and 10 were calculated in proportion to the plant capacities, which are 500 MW (Facilities 2–8) and 1,020 MW (Facilities 9 and 10). Therefore, in this study, the evaluation of Dangjin PP emissions was divided into 2 scenarios:

- Scenario 1: Using only the official CleanSYS data, that is, using emissions from Units 2–8.
- Scenario 2: Adding emissions from generating Units 9 and 10 pilot operations, that is, Scenario 1 plus emissions from Units 9 and 10.

There are 10 coal power facilities in Dangjin PP, as shown in **Figure 5B**. Six stacks are visible since some facilities share stacks. In Scenario 1, 4 stacks were considered as effective stacks in assessment. In Scenario 2, 2 more effective stacks were added for modeling.

- (C) Boryeong PP: Since the DC-8 flew over the top of the stacks, only the emissions of stacks in the upwind side were used, considering wind direction and effective stack heights. In consideration of the effective stack height, only 3 of the 8 stacks were expected to influence the pollution measurements and were used in our analysis. In this plant, LNG and bituminous coal were used as fuel. As shown

Table 1. Estimated NO_x and SO₂ emissions for each LPS

LPS	(A)		(B)		(C)		
	Visible Stacks	Effective Stacks	Visible Stacks	Effective Stacks		Visible Stacks	Effective Stacks
				Scenario 1	Scenario 2		
Number of stacks	8	6	6	4	6	7	3
Fuel types	Anthracite coal, LNG, electricity	Anthracite coal, LNG	Bituminous coal, light oil	Bituminous coal, light oil	Bituminous coal, light oil	Bituminous coal, LNG	Bituminous coal
Data source	CleanSYS	Modified	CleanSYS	Modified	Modified	CleanSYS	Modified
NO _x (Metric ton yr ⁻¹)	6,789	6,600 (97%)*	10,591	10,591 (100%)	15,887 (150%)	6,322	6,219 (98%)
SO ₂ (Metric ton yr ⁻¹)	9,806	9,348 (95%)	4,994	4,994 (100%)	7,491 (150%)	3,860	3,859 (99%)

LNG = liquefied natural gas; LPS = large point source. (A) Hyundai steel mill; (B) Dangjin power plant (PP); (C) Boryeong PP; (D) Seocheon PP; (E) GIC (HanGlas).

*Modified/CleanSYS.

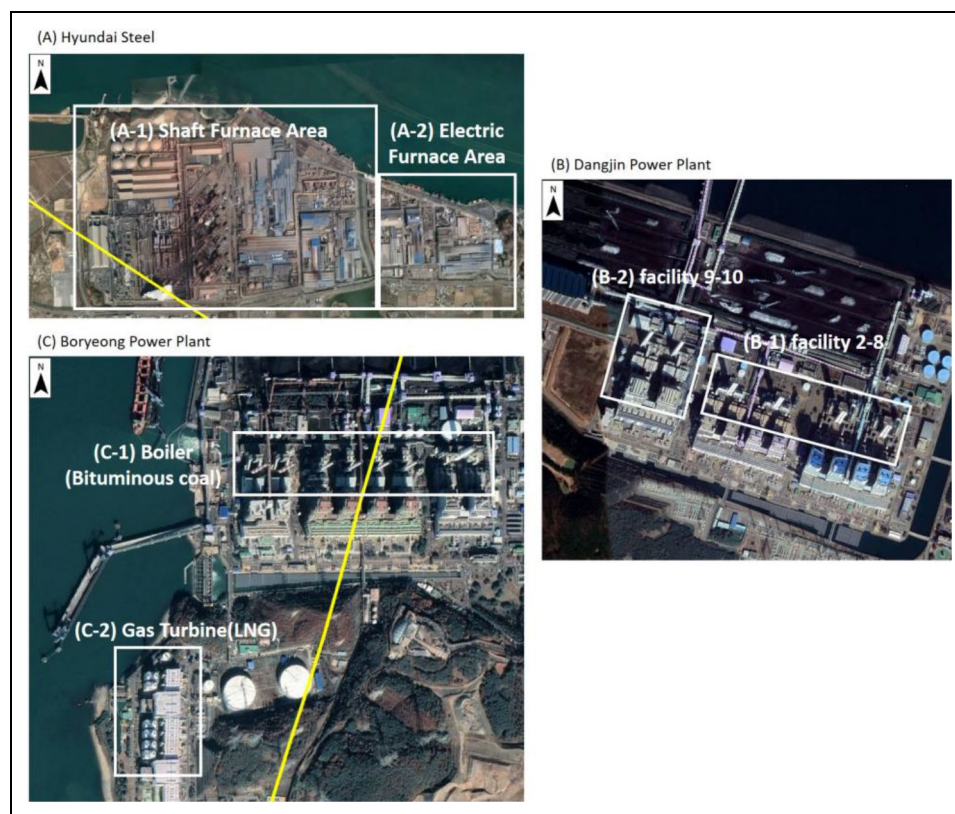


Figure 5. Target sources requiring emission recalculation. White line shows the detail facilities of each selected large point sources, and yellow line shows the DC-8 flight path (June 5). (A) Hyundai steel, (B) Dangjin power plant, and (C) Boryeong power plant.

in **Figure 5C**, Boryeong PP is divided into a boiler area using bituminous coal and a gas turbine area using LNG as fuel. Because the 3 effective stacks are located in the boiler area, emissions from bituminous coal were considered. The emission ratio of bituminous coal accounted for 98% and 99% for NO_x and SO_2 of the total emission of Boryeong PP in the CAPSS inventory, which was used to modify the CleansYS emission.

- (D) Seocheon PP: Because this facility has 1 visible stack and it is an effective stack, emissions did not need to be adjusted.
- (E) GIC (HanGlas): This facility has 3 visible stacks, and also, effective stacks are 3. Those did not need to be adjusted.

4.3. Meteorological data and flight altitude from DC-8 data

Each point along the DC-8 flight path has meteorological measurement data and flight altitude. Meteorological parameters such as temperature, wind direction, and wind speed were measured from the DC-8 aircraft with flight altitude during the flight around the 5 LPSs. By averaging the measurements near each stack, the parameters for the plume model were calculated, which are included in Table S3.

4.4. Stack parameters

Stack parameters such as gas exit velocity, stack gas exit temperature, stack diameter, stack height, and so on for

each LPSs were acquired from the CAPSS 2016. If the sizes of the stacks could be ascertained, such as those in a thermal PP, stack parameters were obtained according to the height of each stack. In cases where the stack height could not be specified, such as Dangjin Hyundai Steel or GIC (HanGlas), all stack information on the site was obtained and averaged, and then, the stack parameters were calculated accordingly. Since the new stacks of the Dangjin thermal PP have different emission conditions from the existing old stacks, the stack parameters were obtained by separating them into old and new. The height of plume rise, ΔH , and effective stack height were calculated using the Holland equation described in Section 3.2.3. based on the above input parameters. All stack parameters for each LPSs are summarized in Table S3.

4.5. Concentrations of pollutants measured from DC-8 aircraft

Pollution measurement data of NO , NO_2 , and SO_2 were employed in our analysis. NO and NO_2 were measured by the “National Center for Atmospheric Research (NCAR) 4-channel chemiluminescence instrument” from the NCAR and SO_2 was measured by the “Georgia Tech-Chemical ionization Mass Spectrometer” from the Georgia Institute of Technology (Weinheimer et al., 1994; Huey et al., 2004; Crawford et al., 2021). Calibration information about NO and NO_2 are in Ryerson et al. (1999) and Ryerson et al. (2000). Those of SO_2 can be found in Chen (2016) and Kim et al. (2007). The reported measurement accuracy for NO

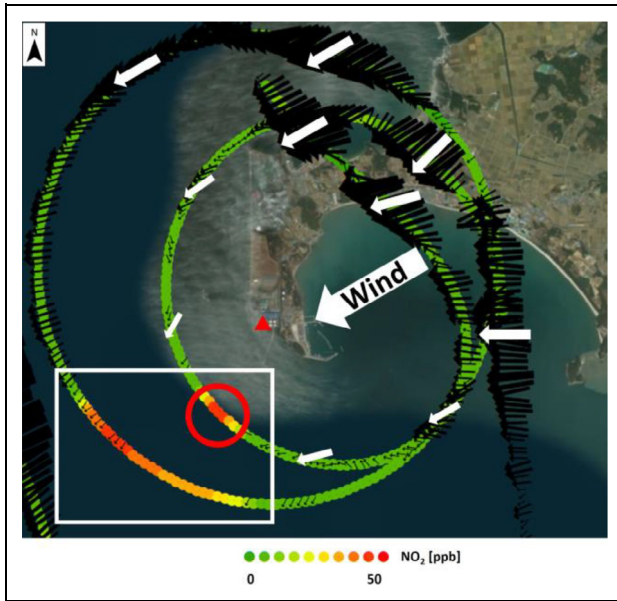


Figure 6. High NO_x concentration area downwind of the Seocheon power plant (PP). The red triangular symbol indicates the location of the Seocheon PP. The red circle indicates data highlighted in **Figure 8**.

and NO₂ by Ryerson et al. (1999) and Ryerson et al. (2000) was 5%. Kim et al. (2007) reported that the measurement accuracy of SO₂ was 10%. NO and NO₂ values were added to determine NO_x concentrations. The influence of background concentration was removed by subtracting the average concentration of measured data, which were not influenced by the designated stack emissions. This method allows a direct comparison of emissions and measured values. The measured concentration data during the flight time period at each LPS are summarized in Table S4.

4.6. Dispersion coefficients

In the Gaussian dispersion model, the dispersion coefficient is a measure of the extent to which the emissions from the source are diffused along their path to the measurement point. The DC-8 measured pollutant concentrations were also used to estimate dispersion coefficients, σ_y and σ_z . The estimation method was described as follows along with the data of Seocheon PP. **Figure 6** shows the NO_x concentrations measured by the DC-8 near the Seocheon PP. The high concentrations of NO_x downwind of the Seocheon PP are located inside the white rectangle of **Figure 6** due to the northeast wind blowing around the stack.

The measured concentration data in the red circle shown in **Figure 6** are plotted by the measurement point number in **Figure 7**. The concentration distributions of NO_x and SO₂ from the DC-8 aircraft show normal distributions. To obtain the dispersion coefficient, the actual atmospheric dispersion coefficient of the Seocheon PP, at the time of the KORUS-AQ measurements, was inversely calculated using this graph (**Figure 7**). It was assumed that most of the pollutants from the stack are included in the range represented by the widest double-headed horizontal arrow in **Figure 7** along with the normal distribution with a reliability of 3 σ (99.7%). Because the aircraft transit

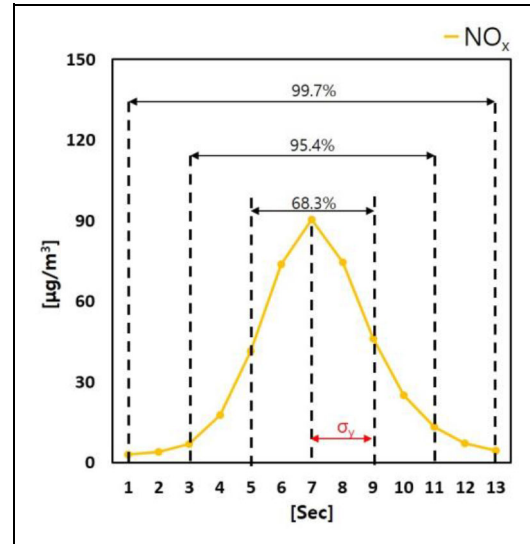


Figure 7. Seocheon power plant NO_x concentrations and dispersion coefficient σ_y . x-axis: time since entering the plume; y-axis: NO_x concentration.

speed was approximately 100 m s⁻¹ and captured measurements by each 1 second, the points in **Figure 6** were converted into 100-m distances. The atmospheric stability at each source was determined by using the formula to estimate the dispersion coefficient that was shown in Table S1. σ_z was calculated by using the confirmed atmospheric stability for each source, distance from each stack, and the factors in Table S1. Estimated σ_y and σ_z values by stability categories A–F for (B) Dangjin PP are shown in Table S5. Values for (A) Hyundai steel mill, (C) Boryeong PP, (D) Seocheon PP, and (E) GIC (HanGlas) are shown in Table S6.

5. Comparisons between measurement and modeled concentration estimates

5.1. Analysis results for PPs: Dangjin, Boryeong, and Seocheon PP

Figure 8 and **Table 2** present the emission estimation results for Dangjin PP. The results from the 2 scenarios at 3 flight points are included. The ratios in **Table 2** are calculated by dividing the sum of the modeled concentrations by the sum of the in-flight measured concentrations. The sum of modeled concentrations was calculated by integrating the area under each curve in **Figure 9**. The closer the ratio is to 1, the better the model results can be judged.

As shown in **Table 2**, the modeled/measured ratios of NO_x and SO₂ in Scenario 1 are less than 1 at BF1, BF2, and BF3 (refer **Figure 4**), which means modeled NO_x and SO₂ emissions were underestimated in this scenario. In Scenario 1, the old 4 stacks were included in the assessment. Two new stacks were added for modeling in Scenario 2. The treatment in Scenario 2 could reduce the bias in the ratio due to the exclusion of pilot operation emissions. As described in the sections above, 2 new facilities in the Dangjin PP complex, which started commercial operation in January 2017, had been in operational testing in mid-2016 during the KORUS-AQ

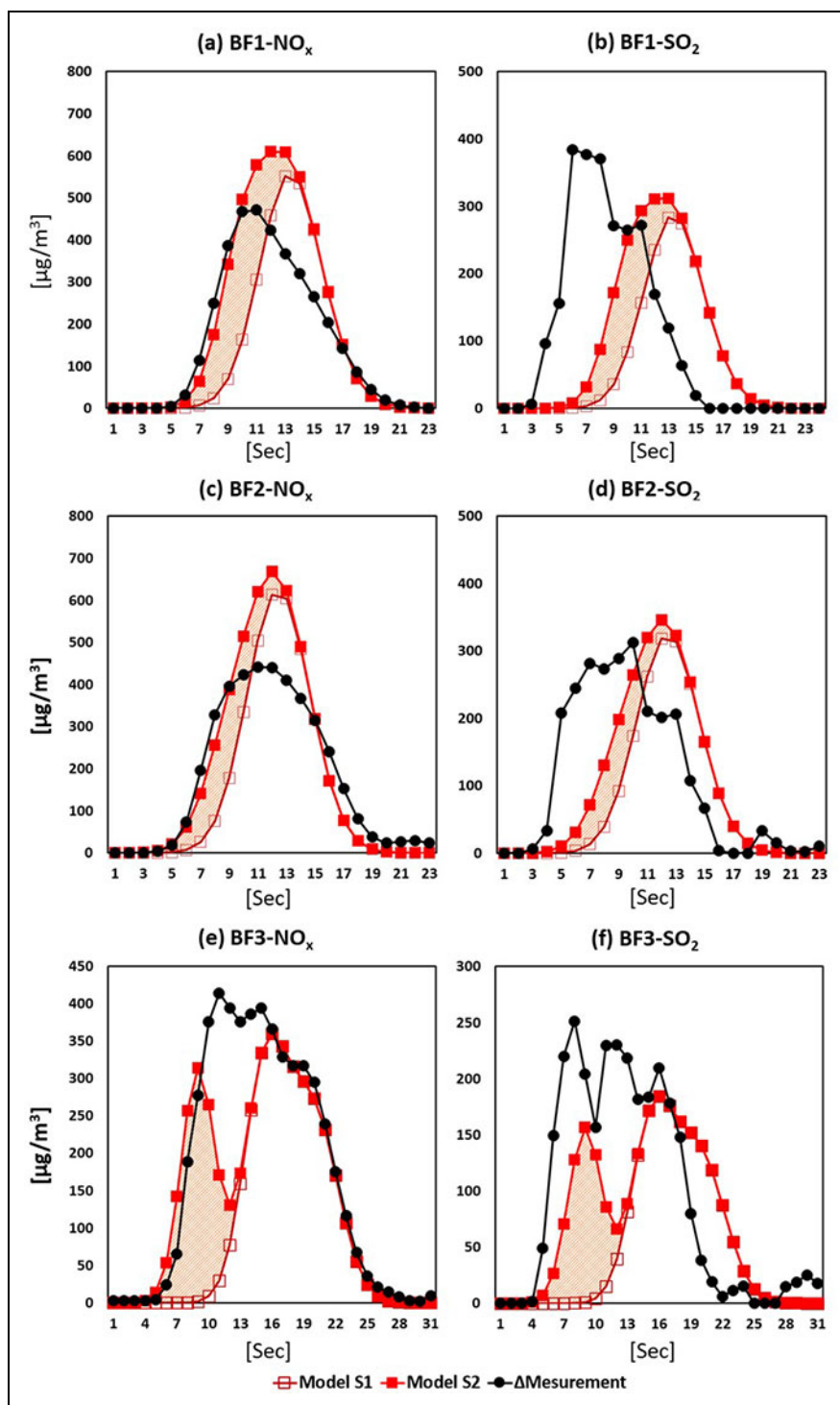


Figure 8. Concentration comparisons in graph between model outcomes and measurements for Dangjin power plant. *x*-axis: time since entering the plume; *y*-axis: concentration. (a) BF1-NO_x, (b) BF1-SO₂, (c) BF2-NO_x, (d) BF2-SO₂, (e) BF3-NO_x, and (f) BF3-SO₂.

Table 2. The ratios of the sum of the modeling concentrations and the sum of the actual concentrations for Dangjin power plant

Measured Point	BF1		BF2		BF3	
	Scenario 1	Scenario 2	Scenario 1	Scenario 2	Scenario 1	Scenario 2
Modeled/measured (NO _x)	0.85	1.22	0.85	1.09	0.59	0.82
Modeled/measured (SO ₂)	0.61	0.87	0.71	0.90	0.56	0.79

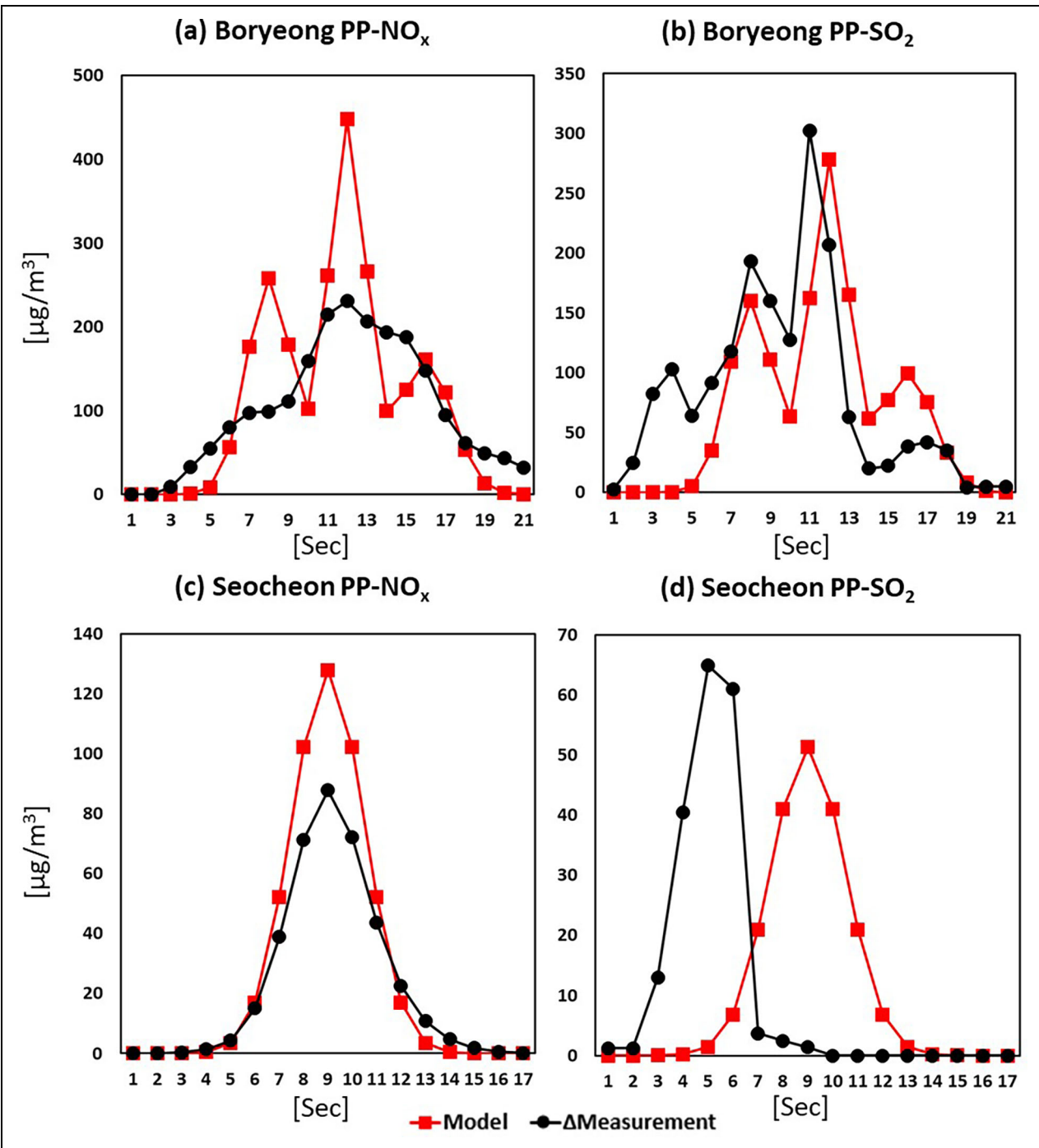


Figure 9. Concentration comparisons in graph between model outcomes and measurements of NO_x and SO₂ for the rest power plant large point sources: (a and b) Boryeong power plant; (c and d) Seocheon power plant. x-axis: time since entering the plume; y-axis: concentration.

measurement campaign. The modeled/measured ratios of NO_x and SO₂ in Scenario 2 are increased and are closer to 1 (Table 2). This means that Scenario 2 performed better emission estimations.

Figure 8e and f depicts the estimated NO_x and SO₂ results from the D3 point. These figures present that the modeled concentrations graph of Scenario 2 has one more peak than those in Scenario 1 due to adding 2 more stacks. In Scenario 1, modeled concentrations at D3 point were estimated to be 0.59 (0.56) times for NO_x (SO₂) compared with in-flight concentration measurements, as

shown in Table 2. When the aircraft flew around the Dangjin PP, the modeled concentration measurements obtained were approximately 60% lower than the in-flight measurements, suggesting the possibility of significant underestimations in the vertically upward emission inventory figures. In Scenario 2, the modeled Dangjin PP concentrations were estimated to be 0.82 (0.79) times for NO_x (SO₂) than those captured in-flight, as shown in Table 2. The emission adjustment in Scenario 2 improved the agreement not only for the amounts but the timing and shapes. Emissions from

Table 3. The ratios of the sum of the modeling concentrations and the sum of the actual concentrations for the rest power plant (PP) large point sources (LPS): Boryeong PP and Seocheon PP

LPS	Boryeong PP	Seocheon PP
Modeled/measured (NO _x)	1.11	1.30
Modeled/measured (SO ₂)	0.85	1.01

the 2 additional stacks were captured by the measurements, and thus, Scenario 2 is considered the more realistic scenario.

Boryeong and Seocheon PP are showing similar results with Dangjing PP. **Figure 9** and **Table 3** show the concentration comparisons results for Boryeong and Seocheon PP. The model-estimated values for NO_x (SO₂) concentrations were 1.11 (0.85) times the measured values for Boryeong PP, where the DC-8 flew over the top of the stack, meaning that the distance between the stack and the measurements was the shortest in this

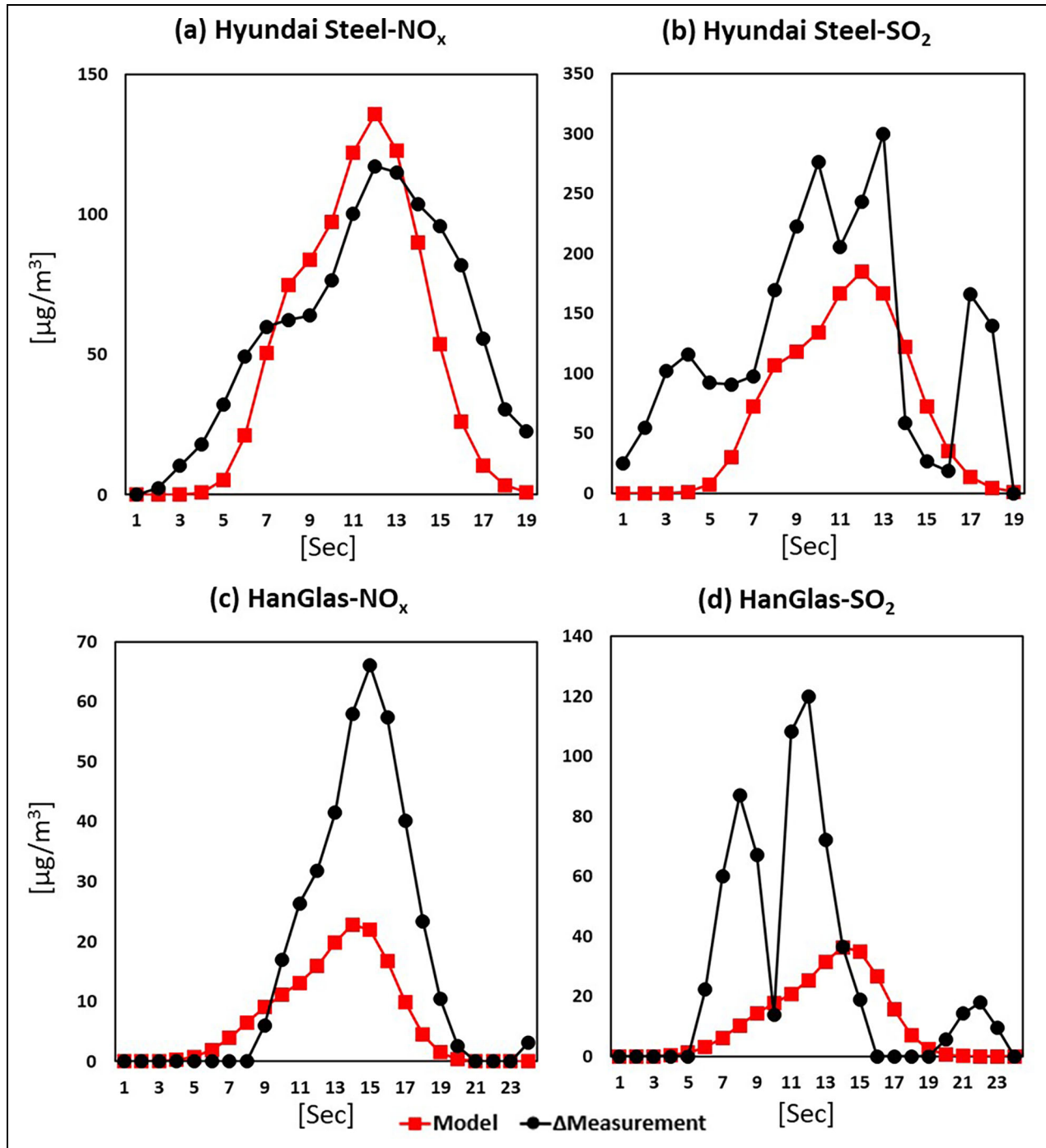


Figure 10. Concentration comparisons in graph between model outcomes and measurements of NO_x and SO₂ for industrial large point sources: (a and b) Hyundai Steel and (c and d) GIC (HanGlas). x-axis: time since entering the plume; y-axis: concentration.

Table 4. The ratios of the sum of the modeling concentrations and the sum of the actual concentrations for the rest power plant large point sources (LPS): Hyundai Steel and GIC (HanGlas)

LPS	Hyundai Steel	GIC (HanGlas)
Modeled/measured (NO _x)	0.82	0.42
Modeled/measured (SO ₂)	0.51	0.39

study. This characteristic means that the Boryeong PP modeled results could be the best match with the measurements. The Seocheon PP was the smallest source evaluated in this study and had just one stack. The modeled Seocheon PP concentrations were estimated to be 1.30 (1.01) times for NO_x (SO₂) compared to the in-flight measurements.

5.2. Industrial sources: Hyundai Steel and Gunsan Industrial Complex (HanGlas)

Air pollutant concentrations (NO_x and SO₂) from the bottom-up emissions driven by the Gaussian plume dispersion model and DC-8 measurement data at each of the remaining industrial LPSs are presented in **Figure 10**. Concentration comparisons for these industrial LPSs are listed in **Table 4**. These results are estimated by the same methodology with other PP sources in Section 5.1.

The model-estimated values for NO_x (SO₂) concentrations were 0.82 (0.51) times the measured values for Hyundai Steel. For GIC (HanGlas), the modeled concentration estimates were 0.42 (0.39) times for NO_x (SO₂) than the values obtained during flight.

As shown in **Table 4**, the matching rates of these 2 sites are lower than those of the PPs shown in **Tables 2** and **3**. As described in Section 4.2, in the concentration modeling of Hyundai Steel and GIC (HanGlas), only the emissions of LPSs whose locations could be identified on satellite maps were used for the input emissions. As described in Section 4.5, emissions from the area sources were attempted to be eliminated because those were considered as background concentrations, but it did not seem to work. The reason seems to be that the flight radius of DC-8 at these sites was so large that it was almost a straight line. As a result, the downwind concentration was measured well, but the upwind concentration was not, and eventually, the flux around the target emission sources could not be fully calculated.

In particular, considering the case of Hyundai Steel, area source emissions account for a large portion of the total emissions from the industrial complex due to the nature of the steel industry. In addition, as shown in **Figure S2**, the area in which the emission sources are distributed is large. Therefore, when estimating the background concentration at this site, a method that can include the influence of area sources is needed. Considering that the distance between the stacks of point sources and the flight

path was close (about 1 km) and the wind direction, in the SO₂ concentration distribution graph of **Figure 10b**, the largest peak in the center can be thought of as the overlapping effect of point source and area source, and it can be thought that only area source emission affected the low peaks on both sides of the graph. Based on this point, the time windows for the background concentration calculation were adjusted (see **Figure S2**). The background concentration was calculated by averaging the concentrations of the time windows on both sides. As a result of comparing the measured concentration corrected with the recalculated background concentration and the modeled concentration, the values in **Table 4** were changed from 0.82 to 1.23 for NO_x and from 0.51 to 0.81 for SO₂, which shows an improvement compared to the results of the previous analysis.

However, as can be seen in **Figure 10**, the measured concentration graph of GIC (HanGlas) shows a strong peak, which is similar to the measured concentration distribution from the LPSs. Therefore, the measured concentration seems to be mainly affected by point sources. In addition, since area source emissions are not significant, it was decided not to correct the effect from the area source emissions. Under this condition, the modeled concentrations appear to be much smaller than the measured concentrations. It could be thought that GIC (HanGlas)'s point source emissions in our national inventory were underestimated than their actual values.

6. Conclusions

In this study, the bottom-up emissions inventory of the LPSs over the mid-west coast of Korea was evaluated for NO_x and SO₂, which cause high levels of PM. Concentrations from a Gaussian plume dispersion model driven by the best available bottom-up emissions and measured meteorological data were intercompared with DC-8 aircraft measurements from circular flights around the emission sources during the KORUS-AQ field campaign. Five LPSs over the mid-west coast of Korea, which are important to improve our understanding of Korean pollution emission sources, were selected for this evaluation.

The input parameters of the GPM were derived from the CAPSS inventory and meteorological measurements on the DC-8 aircraft. Both annual emissions in the inventory and the CleanSYS stack emission measurement data were used to estimate emissions of the selected LPSs to acquire more accurate emissions. The stack parameters such as exit diameter, exit velocity, and exit temperature from the CAPSS point source inventory, and meteorological parameters measured from DC-8, were used to derive the plume rise and dispersion coefficients for the model.

The agreement between modeled and measured concentrations ranged between 0.42 and 1.30 and 0.39 and 1.01 for NO_x and SO₂, respectively. NO_x is overestimated by 4%–30% compared to the ΔMeasurements, which is excluded background concentration at Dangjin PP (BF1 and BF2), Boryeong PP, and Seocheon PP. NO_x at the Hyundai steel, Dangjin PP (BF3), and HanGlas is underestimated by 18%–58% compared to the ΔMeasurements. SO₂ is underestimated by 10%–61% compared to the

Measurements. SO_2 at Seocheon PP is overestimated by 1%. Overall, the NO_x emissions are both underestimated and overestimated for different stacks, whereas the SO_2 emissions are consistently biased low, except for Seocheon PP. These levels of disagreement are, however, not unexpected considering that the modeling results are based on less-than-a-minute measurement snapshots of emissions from the DC-8 compared with 30 min averaged emissions from the CleanSYS.

The possible sources of error in our GPM results are as follows. First, the distance between the stack and the measurements affects the level of agreement. The uncertainty in the model concentrations could decrease as the distance from the stack to the measurements is reduced, as indicated by the best agreement between modeled and measured concentration values from the Boryeong PP where this distance was minimized. The second factor is the complex fuel mix in each facility. In the emissions inventory, complex fuels can cause high variation in the amounts of the emissions. The complex fuels mix, therefore, may cause high model-measurement disagreements. This might be the case with the Seocheon PP, which showed lower agreement. Finally, measurements by the CleanSYS may not reflect additional emissions from the processes in steel mills. In the case of Hyundai Steel, which includes furnace processes for melting iron ore, sintering, and cokes oven, the modeled concentration ratios to the measured values are not in agreement.

Uncertainties in the evaluation could be reduced by adding more detail and realistic emissions. For Dangjin PP, when the emissions were recalculated by adding new facility effects (Scenario 2), modeled concentrations of NO_x and SO_2 were better matched with DC-8 measurement concentrations. The test operations of the newly constructed facility stacks 9 and 10 were underway during KORUS-AQ, and during such a testing period, it could be assumed that these stacks emitted significantly higher pollutant concentrations than during normal commercial operations.

Based on our analysis, the uncertainty of LPS emissions, at least for NO_x and SO_2 , appears to be small, which means point sources inventory emissions in CAPSS seem reasonable. The agreement for the Boryeong PP lends confidence to this conclusion because the measured versus modeled values were 1.11 and 0.85 for NO_x and SO_2 , respectively. Dangjin PP's analysis, however, informs that the more actual and sophisticated emissions should be considered in addition to "the official" amounts to reduce emission uncertainty.

This detailed comparative analysis not only helped in the verification of the national point source emissions inventory for these 2 pollutants (NO_x and SO_2) but also helped in the verification of the method used for this study.

The main purpose of this study was to identify and quantify the problems of the emission inventory by comparing the 2 results from the independent methods, which are observation and Plume modeling. In other words, although the modeled concentration was estimated to describe the measured concentration as

accurately as possible, increasing the agreement rate was not the main purpose of this study. For the purpose of this study, therefore, firstly, in the modeling process, we tried to minimize the uncertainty of plume modeling by calculating the input variables of the plume model and the effective stack heights of point sources by using in situ measured meteorological data. Secondly, in the cases where the target point sources are located in the center of the circular flight path, the effect other than the target pollutant source was removed by deducting the upwind observed concentration from the downwind observed concentration. Through this process, we tried to evaluate the accuracy of the LPS emissions. Third, additionally, based on the understanding of the measured concentration distribution graph, DC-8 flight path, and wind direction, it was attempted to correct and improve the measured concentration of point source emissions from industries such as Hyundai Steel and GCI (HanGlas), where the modeled concentrations were significantly lower than the measured concentration.

The modeled concentrations and measured concentrations of the coal-fired PPs, where most of the emissions are concentrated in LPSs, presented high agreement. This indicates that the verification method proposed in this study was robust and that the inventory emissions of the coal-fired PPs were relatively accurate. In the case of Hyundai Steel, the measured concentration distribution graphs of NO_x and SO_2 were not steep and had a wide peak compared to the graphs of other LPSs. Considering that this is because the influence of area sources was included, the background concentration was recalculated taking into account the measurement time points affected by area sources. As a result, it was possible to sufficiently remove the influence of area source emissions, and it was found that the agreement rates between modeled concentrations and measured concentrations of NO_x and SO_2 were improved by about 20%p and 12%p, respectively. In the case of GIC (HanGlas), the measured concentration distribution graph showed a strong peak which can be seen in the other LPSs, so it needs to be interpreted differently from the case of Hyundai Steel, and it was decided not to correct the effect from the area source emissions since area source emissions are not significant. Therefore, it seemed that GIC (HanGlas)'s point source emissions in our national inventory were underestimated than their actual values.

Inventory assessments using flight measurements will be conducted in the future. The following 2 points are suggested for better analysis in future studies. First, it would be important if the data from the CleanSYS could provide more clear information about the locations of measured stacks. Although there were measured emissions and stack parameters for each stack in the raw data of the CleanSYS, because only the data combined into one location can be received, it was difficult to estimate the exact amount of emissions from each stack. In the case of Hyundai Steel, where the workplace is spatially wide and has various facilities, the sizes of stacks and the amounts of emissions vary. If the location information for each stack in the CleanSYS was provided, better estimation results could have been made. Second, it is expected that

better analysis results will be obtained if the flight measurement time is longer and the flight position and altitude are varied. Except for the Dangjin PP, the number of measurement samples was insufficient. As in the case of the Dangjin PP, it is expected that dispersion coefficients can be estimated better if measurement data are obtained by flying several times at different distances from stacks and flight altitudes. Pollutant concentrations measured at various flight altitudes will provide a better estimate of the centerline of the captured plume. A more comprehensive assumption of the vertical and horizontal distributions of the pollutants will help GPM compute better simulation results. Furthermore, flight measurements over multiple days with various meteorological conditions allow us to verify the accuracy and sensitivity of GPM simulation results by comparing the results of GPM estimations for various conditions.

The experience and findings of this study may help to conduct better inventory assessments in the future. With improved LPS emission inventories through accurate evaluations, it will be possible to accurately predict the occurrence of high concentrations of air pollutants. This leads to implementing appropriate countermeasures, for instance, reducing emissions from some LPSs by adjusting operation time. As a result, public health can be improved by reducing the duration of people's exposure time to hazardous situations.

Data accessibility statement

The Korean CAPSS Emissions inventory are available online at <https://www.air.go.kr/main.do> (last access: November 4, 2022).

The Korean CleanSYS measurement data are available online at <https://cleansys.or.kr/index.do> (last access: November 4, 2022).

The EDGAR data are available online at <https://data.jrc.ec.europa.eu/dataset/377801af-b094-4943-8fdc-f79a7c0c2d19> (last access: November 4, 2022).

The KORUS-AQ aircraft measurements are available online at <https://www-air.larc.nasa.gov/missions/korus-aq/> (last access: November 4, 2022).

Instrument details are available online at <https://impact.earthdata.nasa.gov/casei/campaign/KORUS-AQ#data> (last access: November 4, 2022).

Supplemental files

The supplemental file for this article can be found as follows:

LPS Supplemental Material.docx

Funding

This research was supported by the Fine Particle Research Initiative in East Asia Considering National Differences (FRIEND) Project through the National Research Foundation of Korea (NRF) funded by the Ministry of Science and ICT (2020M3G1A1114621) and by the Korea Environment Industry & Technology Institute (KEITI) through Climate Change R&D Project for New Climate Regime funded by the Korea Ministry of Environment (MOE) (2022003560007).

Competing interests

The authors have declared that no competing interests exist. Isobel J. Simpson is an associate editor at *Elementa*. She was not involved in the review process of this article.

Author contributions

Contributed to conception and design: MP, HH, YK, AF, IJS, J-HW.

Contributed to acquisition of data: HJ, AW, GH, JC.

Contributed to analysis and interpretation of data: MP, HH, YK, AF, IJS, JC, J-HW.

Drafted and/or revised the article: MP, HH, AF, IJS, JC, J-HW.

Approved the submitted version for publication: MP, HH, J-HW.

References

- AirKorea.** 2020. National real-time air pollution open homepage. Available at <https://www.airkorea.or.kr/web>. Accessed November 4, 2022.
- Awasthi, S, Khare, M, Gargava, P.** 2006. General plume dispersion model (GPDM) for point source emission. *Environmental Modeling and Assessment* **11**: 267–276. DOI: <http://dx.doi.org/10.1007/s10666-9041-y>.
- Brunner, D, Kuhlmann, G, Marshall, J, Clément, V, Fuhrer, O, Broquet, G, Löscher, A, Meijer, Y.** 2019. Accounting for the vertical distribution of emissions in atmospheric CO₂ simulation. *Atmospheric Chemistry and Physics* **19**: 4541–4559. DOI: <http://dx.doi.org/10.5194/acp-19-4541-2019>.
- Byun, DW, Ching, JKS.** 1999. *Science algorithms of The EPA MODELS-3 Community Multiscale Air Quality (CMAQ) modeling system*. Washington, DC: U.S. Environmental Protection Agency. EPA/600/R-99/030 (NTIS PB2000-100561).
- Carotenuto, F, Gualtieri, G, Miglietta, F, Riccio, A, Toscano, P, Wohlfahrt, G, Gioli, B.** 2018. Industrial point source CO₂ emission strength estimation with aircraft measurements and dispersion modelling. *Environmental Monitoring Assessment* **190**: 165. DOI: <http://dx.doi.org/10.1007/s10661-018-6531-8>.
- Chen, D, Huey, LG, Tanner, DJ, Salawitch, RJ, Anderson, DC, Wales, PA, Pan, LL, Atlas, EL, Hornbrook, RS, Apel, EC, Blake, NJ, Campos, TL, Donets, V, Flocke, FM, Hall, SR, Hanisco, TF, Hills, AJ, Honomichl, SB, Jensen, JB, Kaser, L, Montzka, DD, Nicely, JM, Reeves, JM, Riemer, DD, Schaufli, SM, Ullmann, K, Weinheimer, AJ, Wolfe, GM.** 2016. Airborne measurements of BrO and the sum of HOBr and Br₂ over the Tropical West Pacific from 1 to 15 km during the CONvective TRANsport of Active Species in the Tropics (CONTRAST) experiment. *Journal of Geophysical Research: Atmospheres* **121**: 12560–12578. DOI: <https://doi.org/10.1002/2016JD025561>.
- Crawford, JH, Ahn, J-Y, Al-Saadi, J, Chang, LS, Emmons, LK, Kim, J, Lee, GW, Park, J-H, Park, RJ, Woo, J-H, Song, C-K, Hong, J-H, Hong, Y-D, Lefer, BL, Lee, MH, Lee, TH, Kim, SW, Min, K-E, Yum, SS, Shin,**

- HJ, Kim, Y-W, Choi, J-S, Park, J-S, Szykman, JJ, Long, RW, Jordan, CE, Simpson, IJ, Fried, A, Dibb, JE, Cho, SY, Kim, YP. 2021. The Korea-United States Air Quality (KORUS-AQ) field study. *Elementa: Science of the Anthropocene* **9**: 1. DOI: <http://dx.doi.org/10.1525/elementa.2020.00163>.
- Crippa, M, Guizzardi, D, Muntean, M, Schaaf, E, Dentener, F, van Aardenne, JA, Monni, S, Doering, U, Olivier, JGJ, Pagliari, V, Janssens-Maenhout, G. 2018. Gridded emissions of air pollutants for the period 1970-2012 within EDGAR v4.3.2. *Earth System Science Data* **10**: 1987–2013. DOI: <http://dx.doi.org/10.5194/essd-10-1987-2018>.
- Crippa, M, Guizzardi, D, Muntean, M, Schaaf, E, Oreggioni, G. 2019. EDGAR v5.0 global air pollutant emissions. European Commission, Joint Research Centre (JRC) [Dataset] PID. Available at <http://data.europa.eu/89h/377801af-b094-4943-8fdc-f79a7c0c2d19>. Accessed June 14, 2023.
- Davenport, AG. 1961. The application of statistical concepts to the wind loading of structures. *Proceedings of the Institution of Civil Engineers* **19**(4): 449–473. DOI: <http://dx.doi.org/10.1680/iicep.1961.11304>.
- De Foy, B, Lu, Z, Streets, DG, Lamsal, LN, Duncan, BN. 2015. Estimates of power plant NO_x emissions and lifetimes from OMI NO₂ satellite retrievals. *Atmospheric Environment* **116**: 1–11. DOI: <http://dx.doi.org/10.1016/j.atmosenv.2015.05.056>.
- Fioletov, VE, McLinden, CA, Krotkov, N, Li, C. 2015. Lifetimes and emissions of SO₂ from point sources estimated from OMI. *Geophysical Research Letters* **42**. DOI: <http://dx.doi.org/10.1002/2015GL063148>.
- Fried, A, Walega, J, Weibring, P, Richter, D, Simpson, IJ, Blake, DR, Blake, NJ, Meinardi, S, Barletta, B, Hughes, SC, Crawford, JH, Diskin, G, Barrick, J, Hair, J, Fenn, M, Wisthaler, A, Mikoviny, T, Woo, J-H, Park, M, Kim, J, Min, K-E, Jeong, S, Wennberg, PO, Kim, MJ, Crouse, JD, Teng, AP, Benett, R, Yang-Martin, M, Shook, MA, Huey, G, Tanner, D, Knote, C, Kim, JH, Park, R, Brune, W. 2020. Airborne formaldehyde and volatile organic compound measurements over the Daesan petrochemical complex on Korea's northwest coast during the Korea-United States Air Quality study: Estimation of emission fluxes and effects on air quality. *Elementa: Science of the Anthropocene* **8**: 1. DOI: <http://dx.doi.org/10.1525/elementa.2020.121>.
- Goldberg, DL, Saide, PE, Lamsal, LN, De Foy, B, Lu, Z, Woo, J-H, Kim, Y, Kim, J, Gao, M, Carmichael, G, Streets, DG. 2019. A top-down assessment using OMI NO₂ suggests an underestimate in the NO_x emissions inventory in Seoul, South Korea, during KORUS-AQ. *Atmospheric Chemistry and Physics* **19**: 1801–1818. DOI: <http://dx.doi.org/10.5194/acp-19-1801-2019>.
- Google Earth Pro 7.3.4.8248. Mid-west region of South Korea. Available at <http://www.google.com/earth/index.html>. Accessed November 4, 2022.
- Grell, GA, Peckham, SE, Schmitz, R, McKeen, SA, Wilczak, J, Eder, B. 2005. Fully coupled “online” chemistry within the WRF model. *Atmospheric Environment* **39**: 6957–6975.
- Han, KM, Lee, S, Chang, LS, Song, CH. 2015. A comparison study between CMAQ-simulated and OMI-retrieved NO₂ columns over East Asia for evaluation of NO_x emission fluxes of INTEX-B, CAPSS, and REAS inventories. *Atmospheric Chemistry and Physics* **15**: 1913–1938. DOI: <http://dx.doi.org/10.5194/acp-15-1913-2015>.
- Holland, JZ. 1953. A meteorological survey of the Oak Ridge area. USAEC Report ORO-99. Oak Ridge, TN: Oak Ridge National Laboratory: 554–559.
- Huey, LG, Tanner, DJ, Slusher, DL, Dibb, JE, Arimoto, R, Chen, G, Davis, D, Buhr, MP, Nowak, JB, Mauldin, RL III, Eisele, FL, Kosciuch, E. 2004. CIMS measurements of HNO₃ and SO₂ at the South Pole during ISCAT 2000. *Atmospheric Environment* **38**(32): 5411–5421. DOI: <http://dx.doi.org/10.1016/j.atmosenv.2004.04.037>.
- Jang, K-W, Lee, J-H, Jung, S-W, Kang, K-H, Hong, J-H. 2009. A study on the comparison of emission factor method and CEMS (Continuous Emission Monitoring System). *Journal of Korean Society for Atmospheric Environment* **25**(5): 410–419. DOI: <http://dx.doi.org/10.5572/KOSAE.2009.25.5.410>.
- Jo, Y-J, Kim, C-H. 2015. Assessment of emission data for improvement of air quality simulation in Ulsan. *Journal of Environmental Impact Assessment* **24**(5): 456–471. DOI: <http://dx.doi.org/10.14249/eia.2015.24.5.456>.
- Kim, B-U, Kim, O, Kim, HC, Kim, S. 2016. Influence of fossil-fuel power plant emissions on the surface fine particulate matter in the Seoul capital area, South Korea. *Journal of the Air & Waste Management Association* **66**(9): 863–873. DOI: <http://dx.doi.org/10.1080/10962247.2016.1175392>.
- Kim, CH, Meng, F, Kajino, M, Lim, JH, Tang, W, Lee, JJ, Kiriya, Y, Woo, J-H, Sato, K, Kitada, T, Minoura, H, Kim, J, Lee, KB, Roh, S, Jo, HY, Jo, YJ. 2021a. Comparative numerical study of PM_{2.5} in exit-and-entrance areas associated with transboundary transport over China, Japan, and Korea. *Atmosphere* **12**: 469. DOI: <http://dx.doi.org/10.3390/atmos12040469>.
- Kim, CH, Park, SY, Kim, YJ, Chang, LS, Song, SK, Moon, YS, Song, CK. 2012. A numerical study on indicators of long-range transport potential for anthropogenic particulate matters over northeast Asia. *Atmospheric Environment* **58**: 35–44. DOI: <http://dx.doi.org/10.1016/j.atmosenv.2011.11.002>.
- Kim, EH, You, SH, Bae, MA, Kang, YH, Son, KW, Kim, ST. 2021b. Municipality-level source apportionment of PM_{2.5} concentrations based on the CAPSS 2016: (IV) Jeollabuk-do. *Journal of Korean Society for Atmospheric Environment* **37**: 292–309. DOI: <https://doi.org/10.5572/KOSAE.2021.37.2.292>.
- Kim, MJ. 2019. The effects of transboundary air pollution from China on ambient air quality in South Korea. *Heliyon* **5**(12). DOI: <http://dx.doi.org/10.1016/j.heliyon.2019.e02953>.

- Kim, NK, Kim, YP, Morino, Y, Kurokawa, J, Ohara, T.** 2013. Verification of NO_x emission inventory over South Korea using sectoral activity data and satellite observation of NO₂ vertical column densities. *Atmospheric Environment* **77**: 496–508. DOI: <http://dx.doi.org/10.1016/j.atmosenv.2013.05.042>.
- Kim, S, Bae, C, Kim, B-U, Kim, HC.** 2017a. PM_{2.5} simulations for the Seoul Metropolitan Area: (I) Contributions of precursor emissions in the 2013 CAPSS Emissions Inventory. *Journal of Korean Society for Atmospheric Environment* **33**(2): 139–158. DOI: <http://dx.doi.org/10.5572/KOSAE.2017.33.2.139>.
- Kim, S, Bae, C, Yoo, C, Kim, B-U, Kim, HC, Moon, N.** 2017b. PM_{2.5} simulations for the Seoul Metropolitan Area: (II) Estimation of self-contributions and emission-to-PM_{2.5} conversion rates for each source category. *Journal of Korean Society for Atmospheric Environment* **33**(4): 377–392. DOI: <http://dx.doi.org/10.5572/KOSAE.2017.33.4.377>.
- Kim, S, Huey, LG, Stickel, RE, Tanner, DJ, Crawford, JH, Olson, JR, Chen, G, Brune, WH, Ren, X, Leshner, R, Wooldridge, PJ, Bertram, TH, Perring, A, Cohen, RC, Lefer, BL, Shetter, RE, Avery, M, Diskin, G, Sokolik, I.** 2007. Measurement of HO₂NO₂ in the free troposphere during the Intercontinental Chemical Transport Experiment–North America 2004. *Journal of Geophysical Research* **112**: D12S01. DOI: <http://dx.doi.org/10.1029/2006JD007676>.
- Kim, S, Kim, O, Kim, B-U, Kim, HC.** 2017c. Impact of emissions from major point sources in Chungcheongnam-do on surface fine particulate matter concentration in the surrounding area. *Journal of Korean Society for Atmospheric Environment* **33**(2): 159–173. DOI: <http://dx.doi.org/10.5572/KOSAE.2017.33.2.159>.
- Kim, S, Moon, N-G, Hong, J-H, Kim, J-Y.** 2009. Source apportionment simulations of NO₂ and ozone concentrations over Seoul Metropolitan Area based on the CAPSS emissions inventory (in Korean). *Journal of Korean Society for Atmospheric Environment*: 280–282. Available at <https://koreascience.kr/article/CFKO200935536012048.pdf>.
- Klimont, Z, Kupiainen, K, Heyes, C, Purohit, P, Cofala, J, Rafaj, P, Borken-Kleefeld, J, Schöpp, W.** 2017. Global anthropogenic emissions of particulate matter including black carbon. *Atmospheric Chemistry and Physics* **17**: 8681–8723. DOI: <http://dx.doi.org/10.5194/acp-17-8681-2017>.
- Korea East-West Power Company.** 2020. About Dangjin Power Plant. Available at <https://ewp.co.kr/eng/main/>. Accessed June 15, 2023.
- Kurokawa, J, Ohara, T.** 2020. Long-term historical trends in air pollutant emissions in Asia: Regional Emission inventory in Asia (REAS) version 3. *Atmospheric Chemistry and Physics* **20**: 12761–12793. DOI: <http://dx.doi.org/10.5194/acp-20-12761-2020>.
- Lavoie, TN, Shepson, PB, Cambaliza, MOL, Stirn, BH, Karion, A, Sweeney, C, Yacovitch, TI, Herndon, SC, Lan, X, Lyon, D.** 2015. Aircraft-based measurements of point source methane emissions in the Barnett Shale Basin. *Environmental Science & Technology* **49**(13): 7904–7913. DOI: <http://dx.doi.org/10.1021/acs.est.5b00410>.
- Lee, C, Martin, RV, van Donkelaar, A, Lee, H, Dickerson, RR, Hains, JC, Krotkov, N, Richter, A, Vinnikov, K, Schwab, JJ.** 2011a. SO₂ emissions and lifetimes: Estimates from inverse modeling using in situ and global, space-based (SCIAMACHY and OMI) observations. *Journal of Geophysical Research* **116**. DOI: <http://dx.doi.org/10.1029/2010JD014758>.
- Lee, DG, Lee, Y-M, Jang, K-W, Yoo, C, Kang, K-H, Lee, J-H, Jung, S-W, Park, J-M, Lee, S-B, Han, J-S, Hong, J-H, Lee, S-J.** 2011b. Korean National Emissions Inventory System and 2007 air pollutant emissions. *Asian Journal of Atmospheric Environment* **5**(4): 278–291. DOI: <http://dx.doi.org/10.5572/ajae.2011.5.4.278>.
- Lee, HM, Park, RJ, Henze, DK, Lee, S, Shim, C, Shin, HJ, Moon, KJ, Woo, J-H.** 2017. PM_{2.5} source attribution for Seoul in May from 2009 to 2013 using GEOS-Chem and its adjoint model. *Environmental Pollution* **221**: 377–384. DOI: <http://dx.doi.org/10.1016/j.envpol.2016.11.088>.
- Lee, Y-M, Lee, H-J, Yoo, C, Song, J-H, Kim, J-Y, Hong, J-H.** 2009. Verification of mobile emission for CMAQ using an observation-based approach in Seoul Metropolitan Area. *Journal of Korean Society for Atmospheric Environment* **25**(5): 369–381. DOI: <http://dx.doi.org/10.5572/KOSAE.2009.25.5.369>.
- Liu, F, Beirle, S, Zhang, Q, Dörner, S, He, K, Wagner, T.** 2016. NO_x lifetimes and emissions of cities and power plants in polluted background estimated by satellite observations. *Atmospheric Chemistry and Physics* **16**: 5283–5298. DOI: <http://dx.doi.org/10.5194/acp-16-5283-2016>.
- Martin, DO.** 1976. Comment on “the change of concentration standard deviations with distance”. *Journal of the Air Pollution Control Association* **26**(2): 145–147. DOI: <https://dx.doi.org/10.1080/00022470.1976.10470238>.
- Ministry of Environment.** 2021. *Handbook of stack remote monitoring system*. Sejong, Korea: ME.
- National Aeronautics and Space Administration.** 2017. KORUS-AQ Flight Summaries. Available at <https://www-air.larc.nasa.gov/missions/korus-aq/index.html>. Accessed November 4, 2022.
- National Aeronautics and Space Administration.** 2020. KORUS-AQ Data Archive. Available at <https://www-air.larc.nasa.gov/cgi-bin/ArcView/korusaq>. Accessed November 4, 2022.
- National Institute of Environmental Research.** 2019. *2016 National Air Pollutants Emission*. Incheon, Korea: NIER.
- National Institute of Environmental Research, National Aeronautics and Space Administration.** 2017. Rapid Science Synthesis Report (RSSR). Available at <https://espo.nasa.gov/sites/default/files/documents/KORUS-AQ-ENG.pdf> (in English); <https://espo.nasa.gov/sites/default/files/documents/KORUS-AQ-RSSR.pdf> (in Korean). Accessed November 17, 2022.

- National Institute of Environmental Research, National Aeronautics and Space Administration.** 2020. KORUS-AQ Final Science Synthesis Report (FSSR). Available at <https://espo.nasa.gov/sites/default/files/documents/5858211.pdf> (in English); <https://espo.nasa.gov/sites/default/files/documents/5858210.pdf> (in Korean). Accessed November 17, 2022.
- Overcamp, TJ.** 1982. A statistical plume model with first-order decay. *Journal of Applied Meteorology* **21**(11): 1589–1593. DOI: [http://dx.doi.org/10.1175/1520-0450\(1982\)021<1589:aspmwf>2.0.co;2](http://dx.doi.org/10.1175/1520-0450(1982)021<1589:aspmwf>2.0.co;2).
- Park, EH, Heo, J, Kim, H, Yi, S-M.** 2020. Long term trends of chemical constituents and source contributions of PM_{2.5} in Seoul. *Chemosphere* **251**: 126371. DOI: <http://dx.doi.org/10.1016/j.chemosphere.2020.126371>.
- Ryerson, TB, Huey, LG, Knapp, K, Neuman, JA, Parrish DD.** 1999. Design and initial characterization of an inlet for gas-phase Noy measurements from aircraft. *Journal of Geophysical Research* **104**(D5): 5483–5492. DOI: <https://doi.org/10.1029/1998JD100087>.
- Ryerson, TB, Williams, EJ, Fehsenfeld, FC.** 2000. An efficient photolysis system for fast-response NO₂ measurements. *Journal of Geophysical Research* **105**(D21): 26447–26461. DOI: <https://doi.org/10.1029/2000JD900389>.
- Shah, V, Jacob, DJ, Li, K, Silvern, RF, Zhai, S, Liu, M, Lin, J, Zhang, Q.** 2020. Effect of changing NO_x lifetime on the seasonality and long-term trends of satellite-observed tropospheric NO₂ columns over China. *Atmospheric Chemistry and Physics* **20**: 1483–1495. DOI: <http://dx.doi.org/10.5194/acp-20-1483-2020>.
- Simpson, IJ, Blake, DR, Blake, NJ, Meinardi, S, Barletta, B, Hughes, SC, Fleming, LT, Crawford, JH, Diskin, GS, Emmons, LK, Fried, A, Guo, H, Peterson, DA, Wisthaler, A, Woo, J-H, Barré, J, Gaubert, B, Kim, J, Kim, MJ, Kim, Y, Knote, C, Mikoviny, T, Pusede, SE, Schroeder, JR, Wang, Y, Wennberg, PO, Zeng, L.** 2020. Characterization, sources and reactivity of volatile organic compounds (VOCs) in Seoul and surrounding regions during KORUS-AQ. *Elementa: Science of the Anthropocene* **8**: 37. DOI: <http://dx.doi.org/10.1525/elementa.434>.
- Statistics Korea.** 2020. National Indicator System. Available at http://www.index.go.kr/potal/main/EachDtlPageDetail.do?idx_cd=1007. Accessed November 4, 2022.
- Touma, JS.** 1977. Dependence of the wind profile power law on stability for various location. *Journal of the Air Pollution Control Association* **27**(9): 863–866. DOI: <http://dx.doi.org/10.1080/00022470.1977.10470503>.
- U.S. Environmental Protection Agency.** 1974. Air Pollution Training Institute: Effective stack height plume rise. SI:406. Available at <https://nepis.epa.gov/Exe/ZyPDF.cgi/91000X85.PDF?Dockey=91000X85.PDF>. Accessed June 14, 2023.
- Weinheimer, AJ, Walega, JG, Ridley, BA, Gary, BL, Blake, DR, Blake, NJ, Rowland, FS, Sachse, GW, Anderson, BE, Collins, JE.** 1994. Meridional distributions of NO_x, NO_y, and other species in the lower stratosphere and upper troposphere during AASE II. *Geophysical Research Letters* **21**: 2583–2586. DOI: <http://dx.doi.org/10.1029/94GL01897>.
- Yeo, MJ, Im, YS, Yoo, SS, Jeon, EM, Kim, YP.** 2019. Long-term trend of PM_{2.5} concentration in Seoul. *Journal of Korean Society for Atmospheric Environment* **35**(4): 438–450. DOI: <http://dx.doi.org/10.5572/KOSAE.2019.35.4.438>.

How to cite this article: Park, M, Hu, H, Kim, Y, Fried, A, Simpson, IJ, Jin, H, Weinheimer, A, Huey, G, Crawford, J, Woo, J-H. 2023. Evaluation of the emission inventory for large point emission sources in South Korea by applying measured data from the NASA/NIER KORUS-AQ aircraft field campaign. *Elementa: Science of the Anthropocene* 11(1). DOI: <https://doi.org/10.1525/elementa.2022.00105>

Domain Editor-in-Chief: Detlev Helmig, Boulder AIR LLC, Boulder, CO, USA

Associate Editor: Md Firoz Khan, Department of Environmental Science and Management, North South University, Dhaka, Bangladesh

Knowledge Domain: Atmospheric Science

Part of an Elementa Special Feature: Korea-United States Air Quality (KORUS-AQ)

Published: July 11, 2023 **Accepted:** May 1, 2023 **Submitted:** August 17, 2022

Copyright: © 2023 The Author(s). This is an open-access article distributed under the terms of the Creative Commons Attribution 4.0 International License (CC-BY 4.0), which permits unrestricted use, distribution, and reproduction in any medium, provided the original author and source are credited. See <http://creativecommons.org/licenses/by/4.0/>.



Elem Sci Anth is a peer-reviewed open access journal published by University of California Press.

OPEN ACCESS The Open Access icon, which is a stylized padlock with a circular arrow around it, indicating that the content is freely available.